Structural Changes of Purple Membrane and Bacteriorhodopsin during Its Denaturation Induced by High pH

Hui Li,[†,‡,§] De-Liang Chen,[†,§] Sheng Zhong,[†] Bing Xu,[†] Bao-Shan Han,[‡] and Kun-Sheng Hu*[,†]

Institute of Biophysics, Chinese Academy of Sciences, Beijing 100101, China, and State Key Laboratory of Magnetism, Institute of Physics, Chinese Academy of Sciences, Beijing 100080, China

Received: October 28, 2004; In Final Form: March 24, 2005

Bacteriorhodopsin (bR) trimers naturally form two-dimensional hexagonal crystals in purple membrane (PM), which make it very stable. However, the dnaturation of bR was found to occur during a very narrow pH range when the pH was increased above 12.0, as indicated by inactivation of the photochemical cycle observed by flash photolysis kinetic spectra. Here, atomic force microscopy was used to study the surface structural changes of PM during the denaturation process induced by high pH. Together with the absorption and fluorescence spectra, it was found that the structural changes could be divided into three steps. First, some hydrophobic amino acids of bR become exposed to the aqueous environment and PM loses its 2D crystalline structure, transforming into the so-called "nonisland" structure. Second, bR molecules are extracted out of membrane and form protrusions on the surface like islands in the sea; therefore, the "nonisland" structure transforms into the "island" structure. Finally, most bRs break off from the membrane and form large depositions.

Introduction

Bacteriorhodopsin (bR), the only protein present in the purple membrane (PM) of *Halobacterium salinarum*, is one of the most extensively studied membrane proteins due to its important biological pump function and its well-established structure.[1] The structure has been determined by X-ray diffraction, electron microscopy, and atomic force microscopy.[2] It consists of seven transmembrane α-helices with a photoactive retinal covalently linked to Lys-216 via a protonated Schiff base.[3,4] In natural PM, bR oligomerizes into trimers, which form two-dimensional (2D) hexagonal crystals. Upon absorption of light, the retinal isomerizes from all-trans to 13-cis, resulting in a structural change in bR and the transport of protons across the PM against the electrochemical gradient. The mechanism of this photochemical cycle and proton pump function of bR and the relationship with its atomic structure is a topic of particular interest. Meanwhile, bR is a promising biomaterial for optoelectronics, optical storage, and information processing.[5,6]

The 2D crystal structure of bR trimers makes PM very stable. Its photocycle ability can be observed upon a wide pH range and at high temperature up to 80 °C.[7] However, the mechanisms that determine protein folding and stability are far beyond fully understood, and it is an important question for understanding the folding of membrane protein and for the future application of PM.[5] The structural stability of bR is dependent on many factors, including intramolecular and intermolecular interactions, protein−lipid interactions, and even protein−retinal interactions.[7] One way to study the stability of protein is to follow its denaturation process upon systematic perturbation of controlled conditions such as detergent, pH, temperature, etc., and to examine the structural changes occurring simultaneously during these transitions.[7] Absorption and circular dichroism (CD) spectra of bR at different values of pH indicate that bR is stable over the pH range 5.0−8.5, while tertiary structural changes occur without secondary structural involvement over the pH range 8.5−11.8.[8,9] Above 11.8, irreversible changes in the membrane organization occur, involving large tertiary and secondary structural changes.[9] The thermal denaturation of bR has also been extensively studied by differential scanning calorimetry (DSC), ultraviolet−visible absorption spectroscopy, CD spectroscopy, and Fourier transform infrared (FTIR) absorption spectroscopy,[7,10,11] as well as X-ray scattering.[12] The main results summarized that bR undergoes a reversible premelting structural transition at 78−80 °C and an irreversible melting transition at about 96 °C, depending on the pH and metal ion concentration.[10,11] However, until now there is no report about the direct observation of PM during denaturation which is supposed to give the firsthand information about the structural changes.

In recent years, atomic force microscopy (AFM) has become an important and powerful tool to study biological samples, due to its ability to image membrane surface topography under controlled aqueous conditions at nanometer resolution. The surface structure of native PM studied by AFM has been reported, and it is possible to discriminate the structural differences between its extracellular surface and cytoplasmic surface.[13] AFM was also used to characterize the structural changes in PM upon illumination[14] and during photobleaching.[15] Together with single molecular force spectrum, AFM has been successfully used to extract an individual bR molecular from the PM[16] and to study the unfolding process of bR.[17] In our former studies, we have used AFM to study the interaction of PM with detergent.[18] All of those experiments demonstrated that AFM could be an ideal method to study the surface structures of PM in different conditions.

However, it is still difficult to image biological samples in liquid with AFM at high temperature due to the thermal drift.

* To whom correspondence should be addressed. Tel.: 86-10-64888580. Fax: 86-10-64877837. E-mail: huks@sun5.ibp.ac.cn.
[†] Institute of Biophysics, Chinese Academy of Sciences.
[‡] Institute of Physics, Chinese Academy of Sciences.
[§] These two authors contributed equally to this paper.

10.1021/jp045087f CCC: $30.25
Published on Web 05/17/2005

An alternative way is to study the denaturation process of bR and PM upon high pH by AFM. In this paper, the denaturation of bR was first characterized by flash photolysis kinetic spectra. AFM was then used to study the surface structural changes of PM during denaturation of bR at high pH. Absorption and fluorescence spectra were used to help the interpretation of the structural changes. The results were further compared with former studies of thermal denaturation of bR.

Materials and Methods

Materials. Culture of the *Halobacterium halobium* and isolation of PM were carried out as described previously.[19,20] Purified PM was suspended in deionized water and stored at 4 °C. The buffer used contained 100 mM KCL and 10 mM glycin, and its pH was adjusted to the desired values using KOH. PM suspension was diluted with the appropriate buffer to a suitable concentration, and the pH was readjusted using KOH.

Flash Photolysis Kinetic Spectra. The flash photolysis kinetic spectra were recorded on our homemade instrument,[21] with the stimulating light at 570 nm wavelength and the probing light at 412 nm wavelength. The final absorption curves were the average of six results, and the data were analyzed using Govindjee's method.[22] The measurements were carried out at room temperature (about 25 °C).

Atomic Force Microscopy. AFM experiments were performed using a commercial microscope (NanoScope IIIa, MultiMode AFM, Digital Instruments). Images were collected with a 13 μm scanner and a liquid cell. Contact mode and tapping mode AFM were used to image the different surface structure. When operated in conact mode, oxide sharpened silicon−nitrogen tips with spring constant of about 0.06 N/m were used. Once tip engaged, a force curve (tip defection vs piezo displacement) was recorded first, and then the setpoint value was adjusted to minimize the force exerted on the sample by tip. Normally, the force was about 100−200 pN. Gains and scan speed were optimized to get the sharpest contrast of images. When operated in tapping mode, we used the oxide sharpened silicon−nitrogen tips with cantilever length of 100 μm and resonance frequency of about 8.5 Hz. The setpoint value was adjusted as maximum as possible to minimize the force and prevent the pollution of tips.

To study the structural changes of PM at high pH, PM samples with different pH values were prepared. A 10 μL aliquot of PM suspension was pipetted onto freshly cleaved mica, left it in air for 3−5 min to allow absorption, and then rinsed with 100 μL of the same buffer to wash off unabsorbed PM. After mounting the sample under the microscopy, 30 μL of the same buffer was injected and the equipment was allowed to stand for 30 min to reach thermal equilibrium.

Images were processed using the software provided with the Nanoscope instrument. First-order flattening and the erase scan line command were performed if needed. The thickness of the membrane was measured using cross-section analysis. The RMS (root-mean-square) value was calculated by the software and taken as an indicator of the surface roughness.

Absorption and Fluorescence Spectra. Absorption spectra were recorded using a Hitachi U-2010 spectrophotometer. Fluorescence spectra were recorded using a Hitachi F-4500 with an excitation wavelength of 280 nm. The measurements were carried out at room temperature (about 25 °C).

Results

Flash Photolysis Kinetic Spectra. The photochemical cycle of bR can be characterized by flash photolysis kinetic spectra

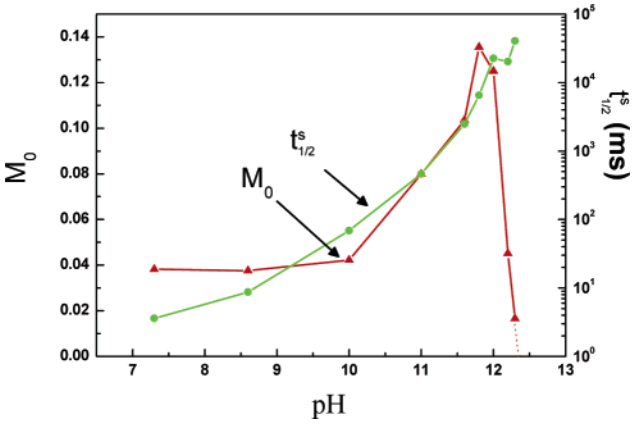

Figure 1. pH-dependent changes in M_0 (relative concentration of M_{412}) and $t_{1/2}^s$ (halftime of slow component of M_{412}) over the pH range 7−12.3.

that represent the decay of one intermediate M_{412} in the photocycle. The curves were fitted to a second-order exponential decay function. It gives the relative concentration of M_{412} (M_0) and the halftimes of the slow and fast components of M_{412} ($t_{1/2}^s$ and $t_{1/2}^f$). However, when pH is higher than 9, only one component of M_{412} ($t_{1/2}^s$) can be characterized. Figure 1 shows the pH-dependent changes in M_0 and $t_{1/2}^s$ over the pH range 7−12.3. M_0 is almost unchanged in the pH range from 7 to 10.0, but there is a large increase in M_0 between pH 10.0 and 11.8. It is caused by a different mechanism of photocycle in pH 10.0−11.8 as compared with the pH range from 7 to 10.0. However, M_0 decreased sharply when the pH rises to 12.0 and became almost undetectable when the pH reaches 12.3. That indicates the photocycle of bR began to be stopped at such a high pH. The changes of $t_{1/2}^s$ elongated extremely above pH 11.8, which also indicated that the photocycle of bR became inactivated. The loss of bR's photocycle upon high pH, in other words, its denaturation, relies on its large structural changes, which is the main topic in the following paragraphs.

Atomic Force Microscopy. AFM was used to image the surface structure of PM in solutions of different pH ranging from 12.0 to 12.6. Images of PM in solution of pH 12.0 were collected by contact mode AFM to obtain highest resolution, as showed in Figure 2. In Figure 2a, several PM sheets were observed with round or elliptical contour and thickness about 5.3 nm, which is almost the same as PM in neutral buffer. The surface topography of one membrane is shown in Figure 2b, in which the 2D hexagonal crystals and the trimer structure can be clearly seen. It is measured that the lattice length is about 6.1 nm, similar to the results of previous studies on PM in neutral buffer.[12,17] We can also conclude that it is the cytoplasmic surface. The results provide strong evidence that the 2D hexagonal crystal and trimer structures of bR are still preserved when the pH is increased to 12.0. However, the circles in Figure 2b outline some areas where bRs seemed to be lost. There are at least two trimers lost within the upper circle and one trimer lost within the circle. There are also some other positions where one or two bR molecules were lost. This phenomenon was hardly observed on PM in solution of neutron pH. So, it is suggested that an increase of pH to 12.0 could induce individual bR or bR trimers extracted from the membrane.

PM samples were further suspended in solutions of pH 12.3 and then imaged by contact mode AFM. Figure 3a shows a typical image in which eight membrane sheets can be observed. We carefully studied the surface structure of every membrane, excluding the membrane at the bottom left corner on which large depositions exist. It is found the membranes can be divided into

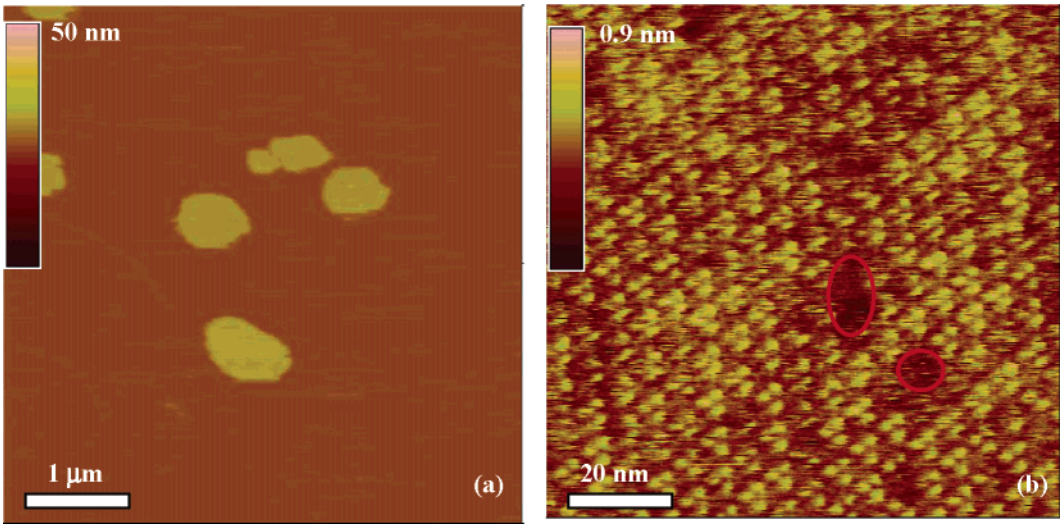

Figure 2. Topographs of purple membrane in solution of pH 12.0. (a) Several PM sheets absorbed onto freshly cleaved mica surface. (b) The membrane surface structure. The 2D hexagonal lattices and trimer structures can be clearly resolved, while the two circles outline areas where bRs were lost.

three types indicated by different arrows in Figure 3a. The dashed arrows point to membranes with relative flat surface, which we termed the "nonisland" structure, while the long solid arrows point to membranes with rough surface, which we term "island" structure, and the short arrow points to a membrane in which the "nonisland" and the "island" structures coexist. The appearance of membranes with different surface structure in one image indicates that PM and bRs are undergoing structural changes under the conditions.

Figure 3b is a high-resolution image of PM with "nonisland" structure. The 2D ordered crystal structure is hardly distinguished. Accompanied by the loss of crystallinity, the surface roughness increases to 0.15 nm (RMS value), as compared with the surface roughness of PM at pH 12.0, which is 0.06 nm. However, the thickness of the membrane (about 5.4 nm) does not show significant change. Moreover, the sporadic bR trimers can be discerned as indicated by the circles, and we supposed some small spots to be individual bR molecules. So, we suggest that in the PM of "nonisland" structures, most bRs lost contact with each other and some bRs partly extended out of the membrane. As consequence, the PM lost its 2D hexagonal lattices, and its surface roughness increased.

Figure 3c shows part of a membrane with "island" structure. The surface of the membrane no longer appears smooth, and there is a large increase in the roughness, as indicated by a RMS value of 0.77 nm. The thickness of the membrane measured at the lowest position is about 5.5 nm, similar to the thickness of PM at pH 12.0, while the thickness measured at the highest position is about 8.1 nm. There appear to be 2.6 nm protrusions extending out of the membrane, like islands out of sea. Hence, we called the feature of Figure 3c the "island" structure. In contrast, we term the surface structure of Figure 3b the "nonisland" structure. In Figure 3c, the protrusions occupy almost half the area of the membrane surface. We attribute the formation of "island" structure to the extraction of bRs from membrane.

Particularly, we found the "nonisland" and "island" structures can be present at one membrane, as indicated by the short arrow in Figure 3a and a more detailed image shown in Figure 3d. The right side of the membrane is the "island" structure just the same as in Figure 3c, while the left side of the membrane appears to be the "nonisland" structure, as its high-resolution topography is the same as in Figure 3b. Using cross-section analysis (Figure 4b), it is measured that the height of the protrusions is about 2.6 nm. The structure of the PM showed no changes during the monitoring period of about half an hour, indicating that the two types of structure are relatively stable. We attribute the coexistence of two structures to the local variance or fluctuation of pH during sample preparation, and it suggests that pH 12.3 is the transforming point of PM from the "nonisland" structure to the "island" structure.

When we tried to image PM at pH 12.6, many large "debris" appear, which are very likely to pollute AFM tips and make imaging difficult. So, we changed to the tapping mode instead of the contact mode to get clear images. Figure 4a shows a typical tapping mode AFM image of PM in solution of pH 12.6. It is showed that many large depositions with height ranging from 10−100 nm appear. We attribute these large depositions to congeries of bRs broken off from membrane. Except for these depositions, there are still membranes that exist with a height of about 5.4 nm. The detailed structure of the membranes is shown in Figure 4b. Its surface roughness is about 0.4 nm, higher than the "nonisland" structure and lower than the "island" structure. We assume these membrane are going from the "nonisland" to the "island" structure.

Absorption and Fluorescence Spectra. To characterize the structural changes associated with the denaturation of bR, absorption and fluorescence spectra were recorded. Figure 5a shows the absorption spectra of bR for the pH range 9.0−12.6. With increasing pH, the wavelength of the absorption peak shows a blue shift from 570 to 550 nm and the absorption maximum decreases, and the peak disappears when the pH reaches 12.6. In addition, at pH 12.3 a peak at 360 nm appears. As dissociated retinal has an absorption maximum at 360 nm, this then indicates that the Shriff base connecting the retinal and Lys216 is broken when the pH rises above 12.3 and retinal begins to be released into the aqueous environment.

Figure 5b shows the fluorescence spectra of PM in buffers of different pH. With the increase of pH from 5.3, the fluorescence spectra do not change until it increased 12.06 when the wavelength of the peak shows a red shift of 6 nm. Also, when the pH is increased to 12.34, the wavelength of the peak was further shifted 10 nm. The consecutive red shifts indicate that the hydrophobic aromatic amino acids of bR exposed to the aqueous environment at two steps. It cannot be determined which aromatic amino acids were involved in each step, but it

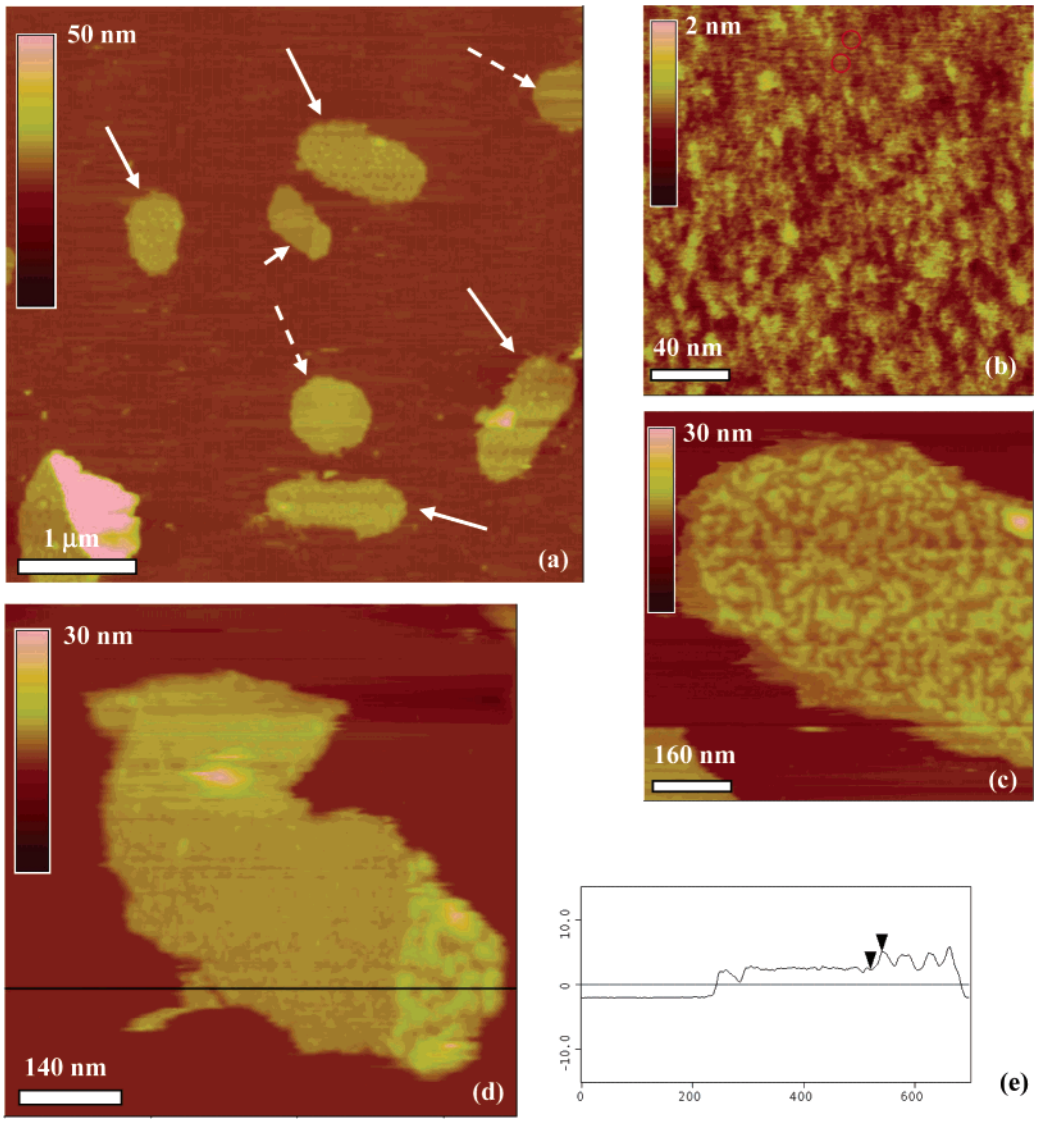

Figure 3. Topographs of purple membrane in solution of pH 12.3. (a) Three kinds of membranes with different surface structures are observed: membranes with a relative flat surface (dashed arrows), membranes with protrusions (solid arrows), and a membrane with two structures coexist (short arrow). (b) Topography of membranes pointed by the dashed arrows, termed "nonisland" structure, shows that the 2D crystal structures have been lost. (c) Topography membrane pointed by the solid arrows, termed "island" structure, shows a much rougher surface with protrusions occupied half area of the membrane. (d) The membrane pointed by short arrow in (a) shows that its left part appears to be a "nonisland" structure and its right part appears to be an "island" structure. (e) Profile of the line in (d) shows that the protrusion is about 2.6 nm high out of the membrane surface.

is assumed that in the second step most hydrophobic amino acids expose to aqueous environment for there are no more changes of fluorescence spectra when pH further increased. As another consequence, the retinal lost protection of hydrophobic amino acids and they are released to the buffer solution as the absorption spectra suggested.

Discussion

The stability of PM depends on the intermolecular and intramolecular interaction of bR, as well as the interaction between bR with the surround lipids. With the increase of pH, the system obtains a large negative charge, which can affect the interactions and lead to protein unfolding and denaturation eventually. Here, we studied the denaturation of bR induced by high pH at room temperature using AFM to characterize the surface structural changes for the first time. Different from the commonly used spectra methods, which give statistical results of many samples, AFM has the ability to study the surface structure of an individual membrane. In such a way, some intermediate states may be observed. Our results show that PMs have different surface structures even in the same conditions. However, there are at least three typical structures during the denaturation of bR induced by high pH ranging from 12.0 to 12.6, as follows:

2D crystal of bR trimer (pH $\leq$ 12.0) $\rightarrow$ "nonisland" structure (12.0 $<$ pH $\leq$ 12.3) $\rightarrow$ "island" structure (12.3 $\leq$ pH $<$ 12.6) $\rightarrow$ large congeries (pH $>$ 12.6).

Our results reveal that in the first step of denaturaton of bR, the 2D crystal structure of PM transforms to the "nonisland" structure over the pH range 12.0−12.3. Over the same pH range, the fluorescence peak shows a 6 nm red shift, indicating that some aromatic amino acids expose to the aqueous environment. So, there must surely be a tertiary structural change that also induces the loss of 2D crystal structure of PM. In Figure 4b, the entire surface loses its 2D crystalline structure. It supports the point that the loss of 2D crystal structure of PM is induced mainly by changes of protein−protein interactions instead of protein−lipid interactions, because it is unlike the detergent

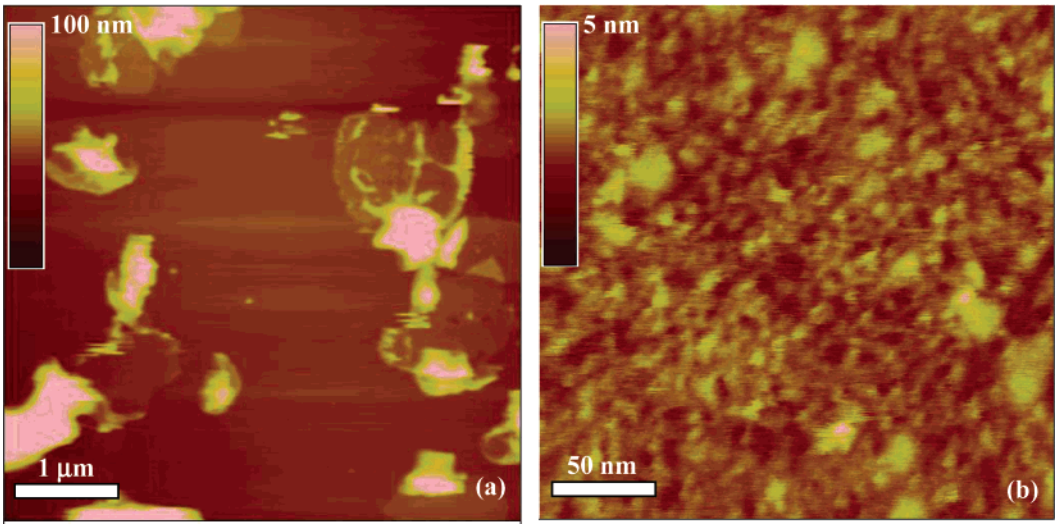

Figure 4. Topographs of purple membrane in solution of pH 12.6. (a) Many large "debris" deposited on the membrane and mica surface. (b) Surface topography of the still existed membranes.

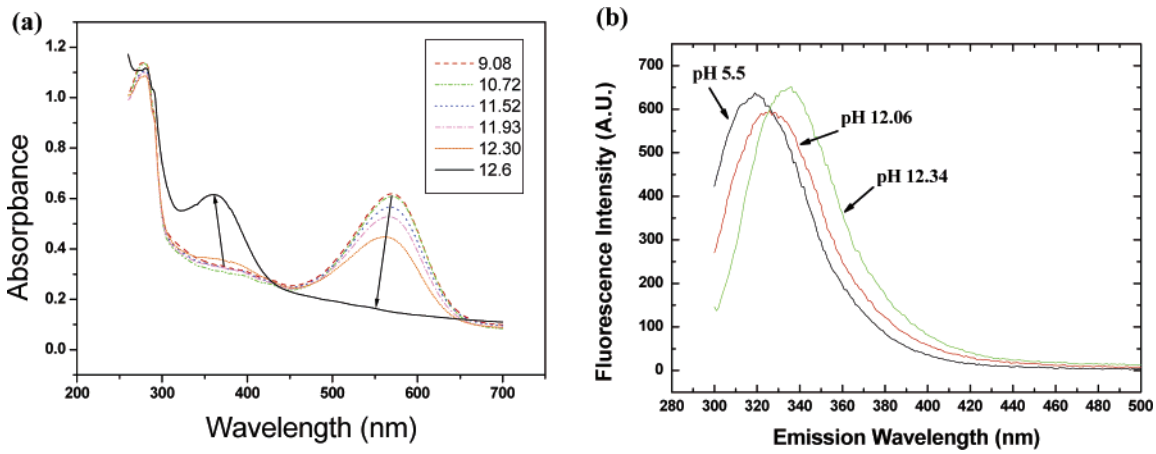

Figure 5. (a) UV−visible absorption spectra of PM in buffers of different pH. (b) Fluorescence spectra of bR in buffers of pH 5.5, 12.06, and 12.34.

solubilization[18] processes, during which detergent molecules insert into membrane and affect the interaction between lipids and protein; as a result, the loss of crystallinity is visible in the form of cracks in the membrane. Studies on the premelting transition during thermal denaturation of bR reveal that the transition is caused by a structural reordering of the crystal lattice, although bR trimer may still persist.[10] X-ray diffraction experiments also indicate that there is a gel-to-liquid transition of the lattice during the premelting transition showing the local order of the trimers is maintained, but the trimeric unit cells are no longer packed in the hexagonal lattice.[12] Therefore, it may suggest that the appearance of "nonisland" structure corresponds to the premelting transition. Also, it might be expected that the "nonisland" structure would convert back to 2D crystal structure if pH is decreased from 12.3 to below 12.0 as the premelting transition is reversible. However, it needs a more precisely environment controlled AFM setup to confirm.

The second step during denaturation is the conversion of PM from "nonisland" to "island" structure with protrusions of about 2.6 nm extending out of the membrane. The protrusions are assumed to be the bR molecules extracted out of the membrane. As a consequence, most hydrophobic amino acids were exposed to aqueous environment as the fluorescence spectra suggested. Meanwhile, the absorption spectra suggest that the retinal break off from bR and are released to buffer solution. In the thermal denaturation study of bR, proteolysis experiments also suggest that bR may be partially extruded from the membrane when undergoing irreversible melting transition.[10] The UV-CD spectroscopy and FT-IR spectroscopy showed that part of bR's α-helical structure was lost and formed random coil in the melting transition.[11] So, it is very likely that the "island" structure was formed by extraction of bR from membrane and lied on the membrane surface in the manner of random coil corresponding to the melting transition, while the membrane still preserved.

The last step during the transition is that bRs break off from membrane and congregate each other to large congeries. At the same pH range, the absorption peak at 500−600 nm disappears, while the absorption at 360 nm increases significantly. This indicates that the retinal has been almost totally released into the buffer solution.

This study demonstrates that AFM is a powerful tool to study structural changes in the PM in liquid at different pH. Further application of AFM to study the PM in situ with more precisely controlled environment, particularly AFM operated at high temperature, may compare the denaturation of bR induced by high pH and the denaturation by high-temperature directly.

Conclusions

Surface structural changes in PM during denaturation of bR induced by high pH can be divided into three steps, as observed

by AFM combined with absorption and fluorescence spectrum. First, some aromatic amino acids become exposed to aqueous environment and the PM loses its 2D crystal structure, converting to the "nonisland" structure. Second, the "nonisland" structure transforms to the "island" structure accompanied by the exposure of most hydrophobic amino acids to the hydrophilic environment and retinal begining to break off from bR. Finally, bRs congregate to large congeries, and the retinal are released into the buffer solution.

Acknowledgment. We thank Dr. Sarah Perrett for helpful discussions. This work was supported by grants from the National Natural Science foundation of China (Grant No. 30170235), the key program of the Chinese Academy of Science (KJ CX1-SW), and the 973 project of the Chinese Ministry of Science and Technology (Grant No. 199801012).

References and Notes

(1) Haupts, U.; Tittor, J.; Oesterhel, D. *Annu. Rev. Biophys. Biomol. Struct.* **1999**, *28*, 367−399.
(2) Heymann, J. B.; Muller, D. J.; Landou, E. M.; Rosenbusch, J. P.; Peyroula, E. P.; Buldt, G.; Engel, A. *J. Stuct. Biol.* **1999**, *128*, 243−249.
(3) Lanyi, J. K. *J. Struct. Biol.* **1998**, *124*, 164−178.
(4) Baudry, J.; Tajkhorshid, E.; Molnar, F.; Philips, J.; Schulten, K. *J. Phys. Chem. B* **2001**, *105*, 905−918.
(5) Hampp, N. *Chem. Rev.* **2000**, *100*, 1755−1776.
(6) Chen, D. L.; Lu, Y. J.; Sui, S. F.; Xu, B.; Hu, K. S. *J. Phys. Chem. B* **2003**, *107*, 3598−3605.
(7) Heyes, C. D.; El-sayed, M. A. *J. Phys. Chem. B* **2003**, *107*, 12045−12053.
(8) Konishi, T.; Hess, B. *FEBS Lett.* **1978**, *92*, 1−4.
(9) Muccio, D. D.; Cassim, J. Y. *J. Mol. Biol.* **1979**, *135*, 595−609.
(10) Brouillette, C. G.; Muccio, D. D.; Finney, T. K. *Biochemistry* **1987**, *26*, 7431−7438.
(11) Heyes, C. D.; El-sayed, M. A. *Biochemistry* **2001**, *40*, 11819−11827.
(12) Muller, J.; Munster, C.; Salditt, T. *Biophys. J.* **2000**, *78*, 3208.
(13) Müller, D. J.; Heymann, J. B.; Oesterhelt, F.; Möller, C.; Gaub, H.; Büdt, G.; Engel, A. *Biochim. Biophys. Acta* **2000**, *1460*, 27−38.
(14) Persike, N.; Pfeiffer, M.; Guchenberger, R.; Fritz, M. *Colloids Surf., B* **2000**, *19*, 325−332.
(15) Möller, C.; Büdt, G.; Dencher, N. A.; Engel, A.; Müller, D. J. *J. Mol. Biol.* **2000**, *301*, 869−879.
(16) Oesterhelt, F.; Oesterhelt, D.; Pfeiffer, M.; Engel, A.; Gaub, H. E.; Müller, D. J. *Science* **2000**, *288*, 143−146.
(17) Müller, D. J.; Kessler, M.; Oesterhelt, F.; Möller, C.; Oesterhelt, D.; Gaub, H. *Biophys. J.* **2002**, *83*, 3578−3588.
(18) Li, H.; Chen, D. L.; Hu, K. S.; Han, B. S. *Chin. Sci. Bull.* **2003**, *48*, 573−476.
(19) Oesterhelt, D.; Stoeckenius, W. *Methods Enzymol.* **1974**, *31*, 667−678.
(20) Xu, B.; Chen, D. L.; Hu, K. S. *Prog. Biochem. Biophys.* **2002**, *29*, 827−831.
(21) Jiang, Q. x.; Hu, K. S.; Shi, H. *Photochem. Photobiol.* **1994**, *60*, 175−168.
(22) Govindjee, R.; Ebrey, T. G.; Crofts, A. R. *Biophys. J.* **1980**, *30*, 231−242.